

Computational DFT Study of ZrSiO₄ Polymorphs: Potential Microelectronic, Nuclear Safety and Geological Implications

Anatoli Korkin,¹ Hideyuki Kamisaka,² Koichi Yamashita,² Andrey Safonov³ and Alexander Bagatur'yants³

¹Nano & Giga Solutions, Gilbert, AZ, ²Department of Chemical System Engineering, The University of Tokyo, Tokyo, Japan, ³Photochemistry center, Russian Academy of Sciences, Moscow, Russia

Zirconium silicate is an extremely durable materials with the variety of useful optical and electronic properties and broad range of existing and potential applications. Using Density Functional Theory (DFT) in local density approximation (LDA) and generalized gradient approximation (GGA) with plane wave (PW) basis set we have revealed eight new polymorphs of ZrSiO₄ within the energy range ~1 eV above the most stable zircon which have higher and lower density than experimentally known zircon and reidite. Two structures, which have both silicon and zirconium atoms six-fold coordinated, orthorhombic AlTaO₄-like (alutomantite) and monoclinic PbWO₄-like (raspite), have similar energies at GGA level ~0.35 eV above reidite and density intermediate between zircon and reidite. Among two low-density structures, which can be potentially revealed experimentally in the nanocrystalline thin films, the orthorhombic CaSO₄-like form has energy similar to reidite but much lower density. We also conducted a comparative study of existing ZrO₂ and SiO₂ polymorphs, which demonstrates the higher accuracy of GGA approach.

Zirconium silicate has a broad range of existing and potential applications such as nuclear safety, microelectronics, protective coating, fuel cells, heterogeneous catalysis and jewelry. Zircon is an extremely durable and resistant material. Its crystalline structure is capable to sustain integrity under a high dose of radiation and accommodate a large quantity of radioactive actinides, which makes it useful as a host material for disposition of nuclear waste.¹ The high optical and mechanical stability of amorphous zirconium silicate films meet the criteria required for the solar coatings application.² Recently, Zr and Hf silicates have drawn considerable attention as alternative [to conventional SiO₂] high permittivity (high-k) gate dielectrics in CMOS devices.³

Besides zircon (group I4₁/amd)⁴ the only other experimentally known form of ZrSiO₄ is reidite,⁵ which belongs to the scheelite (CaWO₄)⁶ type minerals (group I4₁/a) and can be formed from zircon under the static pressure about 12 GPa⁵ and at a higher pressure in the shock wave experiments.⁷ Reidite has a smaller unit cell volume (V_o) and a higher bulk modulus (K_o) than zircon. These two ZrSiO₄ polymorphs have been studied comparatively by Density Functional Theory (DFT)^{8,9} and classical force-field methods.^{8,10} Farnan *et al.*⁹ have reported 6.2 and 11.4 GPa theoretical pressures of the phase transition between two polymorphs at 0°K at the Local Density Approximation (LDA) and Generalized Gradient Approximation (GGA) levels, respectively. Tange and Takahashi¹¹ had observed reidite decomposition to ZrO₂ (cotunnite) and SiO₂ (stishovite) in the pressure range 15-25 GPa and temperature between 1500 and 1800°C. Amorphous zirconium silicate thin films deposited on the silicon substrate also segregate into ZrO₂

and SiO₂ at elevated temperature (>1000°C) applied to anneal the gate stacks in CMOS technology.¹²

Although Reid and Rigwood's work⁵ was motivated by a potential synthesis of a six-coordinated silicate structure, the resulted reidite has four coordinate silicon and eight-coordinated zirconium atoms in its tetragonal unit cell, similar to zircon. No other polymorphous forms of ZrSiO₄ have been reported to our best knowledge, although Guscik et al.¹³ had difficulties in explaining results of their shock wave experiments in the range 0-60 GPA in terms of the phase transformation between zircon and reidite. In amorphous zirconium silicates, which can be produced by vapor deposition, irradiation or melting of the crystalline phase, lower coordination of zirconium atoms was observed (see, for example, ref. 14 and the papers cited therein). In particular, low-coordinated Zr atoms in SiO₂- rich silicates were observed by extended x-ray absorption fine structure spectroscopy (EXAFS) and claimed to cause an enhancement of the dielectric constants of ZrSi_xO_y alloys.¹⁵ (See also ref.16 for a theoretical study of model Zr silicates).

In our paper we studied computationally different ZrSiO₄ polymorphs by using known ABO₄ structures^{17,18} as initial geometries with replaced the A and B cations by Zr and Si atoms and carrying out subsequent optimization of ion positions and the unit cell parameters. DFT computations were carried with LDA VWN¹⁹ and GGA PW91²⁰ along with Vanderbilt ultrasoft pseudopotentials (USPP)²¹ and 29.1 Ry energy cut off. The final GGA calculations presented in our paper were carried using "frozen-core" PAW approach.²² The k points were sampled according to Monkhorst-Pack²³ 4×4×4 scheme. In the calculations of the bulk moduli by fitting P-V in the third-order Birch-Murnaghan equation²⁴ the cut-off energy was increased to 36.4 Ry, and the tetrahedron method with Blöchl correction²⁵ was employed in integration via k-points. All computations were carried out with VASP program package.²⁶

The unique ZrSiO₄ polymorphs revealed in our study within ~1 eV/mol energy range above the most stable zircon structure at LDA or GGA level of theory are presented in the Table 1. They are entitled below by the chemical formulas of the crystalline structures which have been used as starting geometries in ion position and unit cell parameters relaxation. To distinguish them from the original crystalline structures, the corresponding ZrSiO₄ polymorphs are printed in bold letters. In Table 1 we also present the symmetry of the resulting structures, density (at GGA level) and coordination of Zr and Si atoms.

Table 1. ZrSiO₄ polymorphs.

Structure (prototype)	Symmetry	Coordination Zr/Si	Density, g/cm ³ GGA	E(GGA), eV/mol	E(LDA), eV/mol
Zircon	Tetragonal	8/4	4.63	0.0	0.0
CaWO ₄ (Scheelite)	Tetragonal	8/4	5.16	0.43	0.24
SbNbO ₄ (Stibiocolumbite)	Orthorombic	8/4	5.18	0.72	0.58
CaSO ₄ -I (Anhidrite)	Orthorombic	8/4	4.66	0.74	0.84
EuPO ₄ (Monazite)	Monoclinic	8/4	4.91	1.04	0.91
AlTaO ₄ (Alumotantite)	Orthorombic	6/6	4.95	0.78	0.80
PbWO ₄ (Raspite)	Monoclinic	6/6	5.03	0.79	0.75
MnWO ₄ (Wolframite)	Monoclinic	6/6	5.28	1.06	0.82
CaSO ₄ -II (Anhidrite)	Orthorombic	6/4	3.23	0.49	1.05
CuSO ₄ (Chalcocyanite)	Orthorombic	6/4	4.06	0.96	1.39

The first five rows in Table 1 (see also Fig. 1) present the structures which have eight-coordinated Zr and four-coordinated Si atoms in the order of increasing energies. Zircon has the lowest density among the structures with Zr/Si = 8/4 coordination. Molecular volume, bulk moduli and bonds lengths of the two lowest energy experimentally known ZrSiO₄ polymorphs, **zircon** and **CaWO₄** are presented in Table 2 in comparison with experimental and other computational results available in the literature. Three higher energy ZrSiO₄ forms with Zr/Si = 8/4 coordination have been obtained by replacement of the cations and optimization of the orthorhombic SbNbO₄ (stibiocolumbite, group Pc21²⁷ and CaSO₄ (anhydrite, group Amma)²⁸ and monoclinic EuPO₄ (monazite, group P2₁/n)²⁹ (see Fig. 1c, 1d and 1e, respectively). Note, that the rare earth phosphates have both monazite and zircon (xenotime) structures. Monazite preferentially incorporates larger and xenotime smaller cations.²⁹

Remarkably, that at lower energy threshold used in the initial screening we also revealed a low energy monoclinic fergusonite type polymorph (group C2/c), which has been optimized using YNbO₄ structure by replacing Y and Nb atoms by Zr and Si atoms, respectively³⁰ However, with an increased energy threshold and the monoclinic fergusonite **YNbO₄** structure has converged to the tetragonal **CaWO₄**. Transitions between zircon, scheelite and fergusonite type structures under pressure are known for different minerals. Besides zirconium silicate,^{5,7} YVO₄ is also known to undergo an irreversible phase transition from zircon to scheelite structure at 8.5 GPa.³¹ A few ABO₄ minerals, such as CaWO₄,³² CaMoO₄³³ and LiYF₄³⁴ transform from tetragonal scheelite to monoclinic fergusonite structure under pressure above 10-15 GPa.

Table 2 Equilibrium volume at zero pressure and temperature, bulk modulus and bond lengths of the two lowest energy ZrSiO₄ structure, zircon and reidite (CaWO₄ - scheelite) computed at the GGA (LDA) level.

	V ₀ (Å ³)	K ₀ (GPa)	R _{Zr-O} (Å)	R _{Si-O} (Å)
Zircon	263.05 (253.17)	209 (233)	2.266	1.629
	270.4 (256.1)^a	196 (228)^a	2.138	
	Exp.: 263.02^b	Exp.: 227^c		
CaWO₄	236.01 (227.16)	235 (266)	2.256	1.657
	243.2 (229.8)^a	212 (254)^a	2.154	
	Exp.: 235.8^d	Exp.: 301^e		

^{a)} Ref. 9; ^{b)} Ref. 4; ^{c)} Ref. 35; ^{d)} Ref. 5; ^{e)} Ref. 36.

We have revealed three structures, which have both silicon and zirconium atoms six-fold coordinated (see Fig. 2), orthorhombic **AlTaO₄** (alumosilicate, group Pbcn)³⁷ and monoclinic **PbWO₄** (raspite, group P2₁/a)³⁸ and **MnWO₄** (wolframite, group P2/c)³⁹ **AlTaO₄** and **PbWO₄** structures have similar energies at the GGA (within 0.1 eV) and **MnWO₄** polymorph has the highest energy at GGA level and also the highest density among the structures presented in Table 1.

Two low density ZrSiO₄ structures revealed computationally in our study (see last two rows in Table 1) are shown in Fig. 3. The orthorhombic **CaSO₄-II** (Fig. 3a) also originates from the CaSO₄ (anhydrite, group Amma)²⁸ in geometry optimization started from larger c parameter of the unit cell. The two structures, **CaSO₄-I** (see Fig. 1d) and **CaSO₄-II** do not collapsed into each other in LDA and GGA optimization, while they can be converted into each other by compression-expansion of the unit cell along z direction. Compression **CaSO₄-II** increases coordination of Zr atoms from six to eight in **CaSO₄-I**. It is remarkable that **CaSO₄-II** energy at the GGA level is close to the experimentally known reidite, while GGA and LDA results differ significantly. It is apparent from the energies presented in the Table 1 that the low density structures have higher relative energy at the LDA level while opposite trend is revealed for the high density structures. The orthorhombic **CuSO₄** structure (chalcocyanite, group Pnma)⁴⁰ has an intermediate density between **CaSO₄-I** and **CaSO₄-II** structures but higher energy at GGA and LDA levels. The low density metastable nanocrystalline or amorphous structures are likely to be present in zirconium silicates deposited at the low temperature and may result in higher dielectric constants of Zr_xSi_yO_z thin films.¹⁵

In order to estimate accuracy of the DFT methods applied in this study in computation of the relative stability of crystalline of ZrSiO₄ forms we have computed three ZrO₂ (monoclinic, tetragonal and cubic) and three SiO₂ (α-quartz, α-cristobalite, and stishovite) polymorphs for which the numerous experimental and computational results are available (see Table 3). Comparison of our results with experimental thermochemical data and other calculations provides a basis for conclusion that our GGA calculations provide accuracy within ~0.1 eV/mol range (2-3 kcal/mol) while LDA results are certainly less accurate. For both SiO₂ and ZrO₂ LDA has tendency to narrow down the range of energy differences between polymorphs. However, such trend is not present in calculations of ZrSiO₄ polymorphs: Nine structures presented in Table 1 have energy within 1.06 eV at GGA and 1.39 eV at LDA level.

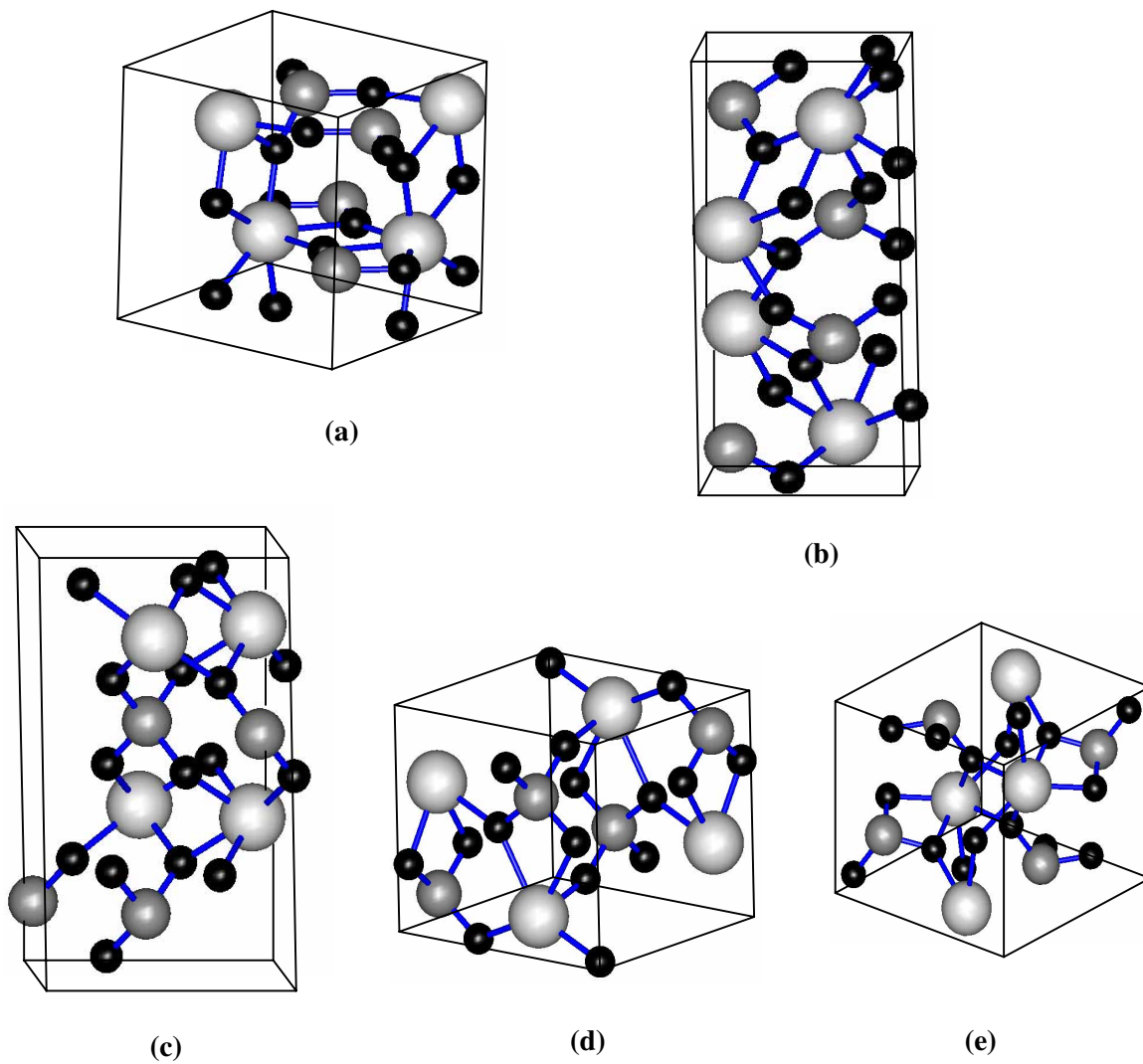
Table 3. Relative energies of SiO₂ and ZrO₂ polymorphs (in eV).

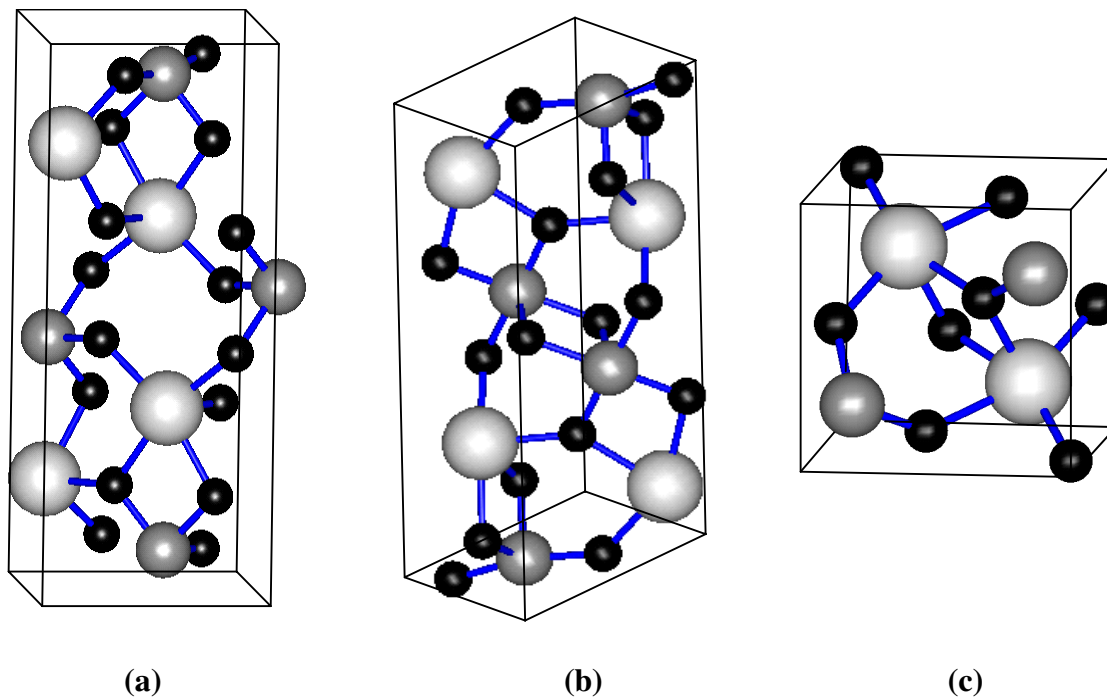
	E (α-quartz) = 0.0		E (m-ZrO₂) = 0	
	(α-cristobalite)	Stishovite	<i>t</i>-ZrO₂	<i>c</i>-ZrO₂
GGA, this study	-0.06	0.53	0.13	0.19
LDA, this study	0.02	0.10	0.04	0.08
Experiment	0.03^a	0.51-0.54^b	0.06^c	0.12^c
GGA		0.57^d	0.11^e	0.17^e
LDA	0.19^f	0.05^f 0.02^d	0.04^e 0.06^g	0.07^e 0.10^g

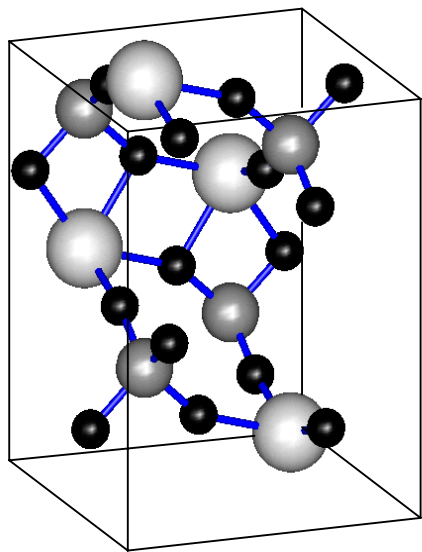
^{a)} Ref. [41], ^{b)} Ref. [42,43], ^{c)} Ref. [44], ^{d)} Ref. [45], ^{e)} Ref. [46], ^{f)} Ref. [47], ^{g)} Ref. [48].

In conclusion we studied computationally virtual polymorphs and found seven new structures of ZrSiO₄ within ~ 1 eV above zircon with the higher and lower density than experimentally known zircon and reidite. Based on the comparison with the available experimental data including those for ZrO₂ and SiO₂ polymorphs we conclude that GGA approach provide more accurate results for energies and structures of ZrSiO₄ polymorphs. Our results should help to identify the potentially existing high and low density ZrSiO₄ polymorphs and in designing novel materials based on it and other ABO₄ minerals. Our future study will focus on a detailed characterization of the new forms of ZrSiO₄ and possibility of their experimental observation and stabilization, e.g. by defects and impurities (dopants). Considering the relatively low energy difference between the experimentally known zircon and reidite structures, the new forms of ZrSiO₄ can be potentially identified at a high pressure, e.g. in the deep mantle, in nano crystalline form at the deposition (low density forms) or in high energy collisions during decay of radioactive ions imbedded in zirconium silicate matrix.

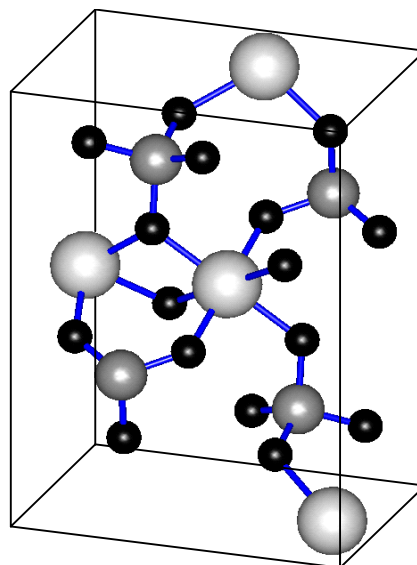
This research was supported by a Grant-in-aid for Scientific Research (KAKENHI) in Priority Area "Molecular Nano Dynamics", from the Ministry of Education, Culture, Sports, Science and Technology of Japan. The authors thank the Computer Center of the Institute for Molecular Science for the use of computers.

**Fig. 1**

**Fig. 2**



(a)



(b)

Fig. 3

-
- ¹R. C. Erwing, W. Luize, and W.J. Weber, *J. Mater. Res.* **10**, 243 (1995); A. Meldrum, L.A. Boatner, W.J. Weber, and R.C. Erwing, *Geochem. Cosmochem. Acta* **62**, 2509 (1998); R.C. Erwing, *Proc. Natl. Acad. Sci.* **96**, 3432 (1999).
- ²E. Ando, J. Ebisawa, Y. Hayashi, A. Mitsui, S. Suzuki, *J. Non-Crystalline Solids* **178** (1994) 238.
- ³G. Wilk, R.W. Wallace, J.M. Anthony, *J. Appl. Phys.* **89** (2001) 5234.
- ⁴S. Rios, T. Malcherek, E.K.H. Salje, C. Domeneghetti, *Acta Cryst.* **B56**, 947 (2000).
- ⁵A.F. Reid and A.E. Ringwood, *Earth. Planet. Sci. Lett.* **6**, 205 (1969); L.G. Liu, *ibid* **44**, 390 (1979).
- ⁶A. Zalkin, D.N. Templeton, *J. Chem. Phys.*, **40**, 501 (1964); M.I. Kay, B.C. Frazer, I. Almodovar, *Ibid.* **40**, 504 (1964).
- ⁷K. Kusaba, T. Yagi, M. Kikuchi, and Y. Syono, *J. Phys. Chem. Solids* **47**, 675 (1986).
- ⁸J.-P. Crocombette and D. Ghaleb, *J. Nuc. Mat.* **257**, 282 (1998)
- ⁹I. Farnan, E. Balan, C.J. Pickard, and F. Mauri, *Am. Mineralogist* **88**, 1663 (2003).
- ¹⁰M.J. Akhtar, and S. Waseem, *Solid State Sci.* **5**, 541 (2003).
- ¹¹Y. Tange and E. Takahashi, *Phys. Earth Planet. Inter.* **143-144**, 223 (2004).
- ¹²S. Stemmer, D.G. Schlom, In *Nano and Giga Challenges in Microelectronics*, edited by J. Greer, A.Korkin and J. Labanowski (Elsevier, Amsterdam, 2003), p. 129.
- ¹³A. Gucsik, C. Koeberl, F. Brandstätter, W.U. Reimold, and E. Libowitzky, *Earth Planet. Sci. Lett.* **202**, 495 (2002).
- ¹⁴E. Balan, F. Mauri, C.J. Pickard, I. Farnan, and G. Calas, *Am. Mineralogist*, **88**, 1769 (2003).
- ¹⁵G. Lucovsky, and G.B. Rayner, Jr., *Appl. Phys. Lett.* **77**, 2912 (2000).
- ¹⁶G.-N. Rignanese, F. Detraux, X. Gonze, A. Bongiorno, A. Pasquarello, *Phys. Rev. Lett.* **89**, 117601 (2002).
- ¹⁷<http://database.iem.ac.ru/mincryst/> (Crystallographic and Crystallochemical Database for Mineral and their Structural Analogues).
- ¹⁸<http://webmineral.com/> (Minerology Database)
- ¹⁹D. M. Ceperley and B. J. Adler, *Phys. Rev. Lett.* **45**, 566 (1980); S. J. Vosko, L. Wilk and M Nusair, *Can. J. Phys.* **58**, 1200 (1980).
- ²⁰J. P. Perdew, J. A. Chevary, S. H. Vosko, K. A. Jackson, M.R. Pederson, D. J. Singh and C. Fiolhais, *Phys. Rev. B* **46**, 6671 (1992); J. P. Perdew and Y. Wang, *Phys. Rev. B* **45**, 13244 (1992).
- ²¹D. Vanderbilt, *Phys. Rev. B* **85**, 7892 (1990); G. Kresse and J. Hafner, *J. Phys.: Condens. Matter* **6**, 8245 (1994).
- ²²P. E. Blöchl, *Phys. Rev. B* **50**, 17953 (1994); G. Kresse and D. Joubert, *Phys. Rev B* **59**, 1758 (1999).
- ²³H. J. Monkhorst and J. D. Pack, *Phys. Rev. B* **13**, 5188 (1976).
- ²⁴F. D. Murnaghan, *Proc. Natl. Acad. Sci.* **30**, 244 (1944); F. Birch, *J. Geophys. Res.* **83**, 1257 (1978).
- ²⁵O. Jepsen and O. K. Anderson, *Solid State Commun.* **9**, 1763 (1971); P. E. Blöchl, O. Jepsen and O. K. Andersen, *Phys. Rev. B* **49**, 16223 (1994).

-
- ²⁶Vienna *ab initio* simulation package (VASP); Version 4.4.5 ;
<http://cms.mpi.univie.ac.at/vasp/>. See also G. Kresse and J. Furthmüller, *Comput. Mater. Sci.*, **6**, 4136 (1996).
- ²⁷R.S. Roth and J.L. Waring, *Am. Mineralogist* **48**, 1348 (1963).
- ²⁸F.C. Hawthorne and R.B. Ferguson, *Canad. Mineral.* **13**, 289 (1975).
- ²⁹Y. Ni, J.M. Hughes, and A.N. Mariano, *Am. Mineralogist* **80**, 21 (1995).
- ³⁰H. Weitzel and H. Schrocke, *Z. Kristallogr.* **152**, 69 (1980).
- ³¹X. Wang, I. Loa, K. Syassen, M. Hanfland, and B. Ferrand, *Phys. Rev. B* **70**, 064109 (2004)
- ³²A. Grzechnik, W.A. Crichton, M. Hanfland, and S. van Smaalen, *J. Phys.: Condens. Matter* **15**, 7261 (2003)
- ³³W.A. Crichton and A. Grzechnik, *Z. Kristallogr. NCS* **219**, 337 (2004).
- ³⁴A. Grzechnik, K. Syassen, I. Loa, M. Hanfland, and J.Y. Gesland, *Phys. Rev. B* **65**, 104102 (2002); J. Manion, S. Jandl, K. Syassen, and J.Y. Gesland, *Phys. Rev. B* **64**, 235108 (2002).
- ³⁵R.M. Hazen and L.W. Finger, *Amer. Mineral.* **64**, 196 (1979).
- ³⁶H.P. Scott, Q. Williams, and E. Knittle, **88**, 15506 (2002).
- ³⁷T. S. Ercit, F.C. Hawthorne, and P. Cerny, *Canad. Mineral.*, **30**, 653 (1992).
- ³⁸T. Fujita, J. Kawada, and K. Kato, *Acta Cryst.* **B33**, 162 (1977).
- ³⁹H. Weitzel, *Z. Kristallogr.* **144**, 238(1976).
- ⁴⁰M. Wilder and G. Giester, *Mineralogy and Petrology*, **39**, 201 (1988).
- ⁴¹I. Petrovic, P.J. Heaney, and A. Navrotsky, *Phys. Chem. Minerals* **23**, 119 (1996).
- ⁴²J.L. Holm, O.J. Kleppa, and E.E. Westrum, Jr. *Geochim. Cosmochim. Acta* **31**, 2289 (1967).
- ⁴³M. Akaogi, and A. Navrotsky, *Phys. Earth. Planet. Inter.* **36**, 124 (1984).
- ⁴⁴R. Ackerman, E. G. Rauh, and C. A. Alexander, *High Temp. Sci.* **7**, 304 (1975).
- ⁴⁵D.R. Hamann, *Phys. Rev. Lett.* **76**, 660 (1996).
- ⁴⁶J.E. Jaffe, R.A. Bacher, and M. Gutowski, *Phys. Rev. B* **72**, 144107 (2005).
- ⁴⁷N.R. Keskar, and J. R. Chelikowsky, *Phys. Rev. B.* **46**, 1 (1992).
- ⁴⁸B. Králik, E. K. Chang and S. G. Louie, *Phys. Rev. B* **57**, 7027 (1998).

Figure captions

Fig. 1. Crystalline structures of the ZrSiO_4 polymorphs containing eight-coordinated Zr and four-coordinated Si atoms (GGA results): (a) tetragonal zircon: $a = b = 6.631 \text{ \AA}$, $c = 5.983 \text{ \AA}$; (b) tetragonal **CaWO₄**: $a = b = 4.743 \text{ \AA}$, $c = 10.492 \text{ \AA}$; (c) orthorhombic **SbNbO₄**: $a = 5.101 \text{ \AA}$, $b = 5.083 \text{ \AA}$, $c = 9.058 \text{ \AA}$; (d) orthorhombic **CaSO₄-I**: $a = 6.594 \text{ \AA}$, $b = 6.634 \text{ \AA}$, $c = 5.972 \text{ \AA}$; (e) monoclinic **EuPO₄**: $a = 6.241 \text{ \AA}$, $b = 6.554 \text{ \AA}$, $c = 6.302 \text{ \AA}$, $\beta = 105.8^\circ$; Zr – Large light grey circles, Si – smaller dark grey circles, and O- small black circles.

Fig. 2. Crystalline structures of ZrSiO_4 polymorphs which have six-coordinated Zr and Si atoms (GGA results): (a) orthorhombic **AlTaO₄**: $a = 4.695 \text{ \AA}$, $b = 11.241 \text{ \AA}$, $c = 4.661 \text{ \AA}$; (b) monoclinic **PbWO₄**: $a = 11.779 \text{ \AA}$, $b = 4.610 \text{ \AA}$, $c = 4.725 \text{ \AA}$, $\beta = 109.2^\circ$; (c) monoclinic **MnWO₄**: $a = 4.684 \text{ \AA}$, $b = 5.081 \text{ \AA}$, $c = 4.907 \text{ \AA}$, $\beta = 98.8^\circ$. Zr – Large light grey circles, Si – smaller dark grey circles, and O- small black circles.

Fig. 3. Crystalline structures of low density ZrSiO_4 polymorphs (GGA results): (a) orthorhombic **CaSO₄-II**: $a = 6.420 \text{ \AA}$, $b = 6.561 \text{ \AA}$, $c = 8.944 \text{ \AA}$; (b) orthorhombic **CuSO₄**: $a = 9.115 \text{ \AA}$, $b = 6.790 \text{ \AA}$, $c = 4.850 \text{ \AA}$. Zr – Large light grey circles, Si – smaller dark grey circles, and O- small black circles.